Atmos. Chem. Phys. Discuss., https://doi.org/10.5194/acp-2018-1345
Manuscript under review for journal Atmos. Chem. Phys.
Discussion started: 23 January 2019

Atmospheric Chemistry and Physics Discussions

Characterizations and source analysis of atmospheric inorganic ions at a national background site in the northeastern Qinghai-Tibet Plateau: insights into the influence of anthropogenic emissions on a high-altitude area of China

Bin Han[1], Jing Wang[1], Xueyan Zhao[1], Baohui Yin[1], Xinhua Wang[1], Xiaoyan Dou[2], Wen Yang[1], Zhipeng Bai[1]

1. State Key Laboratory of Environmental Criteria and Risk Assessment, Chinese Research Academy of Environmental Sciences, Beijing, China
2. Qinghai Environmental Monitoring Center, Xining, Qinghai, China

Abstract

Atmospheric particulate matter (PM) imposes highly uncertain impacts on both radiative forcing and human health. While ambient PM has been comprehensively characterized in China's megacities; its composition, source, and characteristics in the Qinghai-Tibet Plateau (QTP) are not yet fully understood. An autumn observational campaign was conducted during the 1st - 15th October 2013 at a national background monitoring station (3295 m a.s.l.) in the QTP. Real time concentrations of inorganic water-soluble ions (WSIs) associated with $PM_{2.5}$ were measured in addition to $PM_{2.5}$ concentrations, gaseous pollutants, and meteorological parameters. SO_4^{2-} was the most abundant WSI (10.00 ±4.39 μg/m^3) followed by NH_4^+ (2.02 ±0.93 μg/m^3), and NO_3^- (1.65 ±0.71 μg/m^3). Observed WSI concentrations were lower as compared to urban sites in eastern China; however, they were higher as compared to other QTP monitoring sites. High sulfate and nitrate oxidation ratios indicated strong secondary formation of both SO_4^{2-} and NO_3^-. Both photochemical and heterogeneous reactions contributed to the formation of particulate SO_4^{2-}, while the conversion of NO_2 to NO_3^- only occurred via photochemical reactions in the presence of high O_3 concentrations and strong sunlight. Correlation analysis between WSIs revealed that NH_4NO_3, $(NH_4)_2SO_4$, Na_2SO_4, and K_2SO_4 were the major atmospheric aerosol components. To better understand the potential sources of WSIs in the QTP, a Positive Matrix Factorization receptor model was used. Results showed that salt lake emissions, mixed factor emissions (livestock feces emission, occasional biomass burning, and crustal material), traffic emissions, secondary inorganic aerosols, and residential burning were the major emission sources at the study site.

Atmos. Chem. Phys. Discuss., https://doi.org/10.5194/acp-2018-1345
Manuscript under review for journal Atmos. Chem. Phys.
Discussion started: 23 January 2019

Atmospheric Chemistry and Physics Discussions

1. Introduction

Atmospheric aerosol has a significant impact on climate change and human health, the extent of which is determined by their physical and chemical properties. High concentrations of aerosols are associated with rapid economic growth, urbanization, industrialization, and motorization, and have become a major environmental concern in China (Du et al., 2015). Extensive research has investigated the sources, chemical and physical properties, and evolution processes of aerosol particles at urban and rural sites in China during the last decade (Cao et al., 2007; Gong et al., 2012; He et al., 2011; Jiang et al., 2015; Sun et al., 2015; Sun et al., 2013; Wu et al., 2007b). These studies indicated that fine particles are mainly composed of organics, sulfate, nitrate, ammonium, mineral dust, and black carbon. While these studies have greatly improved our understanding on the sources and physical/chemical properties of aerosol particles, they were predominantly conducted in developed areas of China, including Beijing–Tianjin–Hebei, the Pearl River Delta, and the Yangtze River Delta. In remote areas, such as the Qinghai-Tibet Plateau (QTP), studies on atmospheric aerosol properties are rare.

The QTP covers most of the Tibet Autonomous Region and Qinghai Province in western China, with an area of 5,000,000 km^2 and an average elevation over 4000 m. The area is geomorphologically the largest and highest mountain region on earth (Yao et al., 2012). Described as the "water tower" of Asia, this area contains the headwaters of the Mekong, Yangtze, and Yellow Rivers. Therefore, climate variability and change in this region has fundamental impacts on a range of climate-related ecosystem services (McGregor, 2016). Due to its unique ecosystem, landforms, and monsoon circulation, the QTP has a profound role in regional and global atmospheric circulation, radiative budgets, and climate systems (Su et al., 2013; Kopacz et al., 2011; Yang et al., 2014; Jin et al., 2005). Limited anthropogenic activity, a sparse population, immense area, and high elevation mean that, alongside the Arctic and Antarctic, the QTP is considered one of the most pristine terrestrial regions in the world. Because of this, the region is an ideal location for characterizing background aerosol properties, regional and global radiative forcing, climate and ecological changes, and the transportation of global air pollutants. Thus, a comprehensive understanding of QTP aerosol chemistry is crucial for assessing anthropogenic influences and evaluating long-term changes in the global environment (Cong et al., 2015; Zhang et al., 2012).

Research relating to the chemical and physical characteristics of aerosols in the QTP is rare; hence, their sources, properties, and evolution processes are poorly understood. This lack of research is a result of the region's remoteness and challenging weather conditions. Most previous studies of aerosol chemistry in the QTP were conducted in the Himalaya (the southeastern or southern areas of the QTP) to assess the key roles of the Himalaya on regional climate and the environment, as well as the boundary transportation of air pollutants from South Asia (Cong et al., 2015; Zhao et al., 2013b; Wan et al., 2015; Shen et al., 2015). Conversely, the northeastern QTP, located in inland China, is likely to have very different atmospheric

Atmos. Chem. Phys. Discuss., https://doi.org/10.5194/acp-2018-1345
Manuscript under review for journal Atmos. Chem. Phys.
Discussion started: 23 January 2019

behaviors as compared to those of the Himalaya due to different climate patterns and aerosol sources between the two regions (Xu et al., 2015). Several studies in the northeastern QTP found that SO_4^{2-}, NO_3^-, NH_4^+, and Ca^{2+} were major water-soluble ions (WSIs), suggesting that both anthropogenic pollution and mineral dust contributed to the total mass of $PM_{2.5}$ (Xu et al., 2014; Li et al., 2013; Zhang et al., 2014). Du et al. (2015) also found that sulfate and ammonium were dominant in PM_1 mass in this area. Other studies from the Waliguan Observatory (36°17'N, 100°54'E, 3816 m a.s.l.), a land-based Global Atmosphere Watch (GAW) baseline station, located in the northeast of the Tibetan Plateau, found that particles at this site were predominantly from natural sources, such as soil and crust (Wen et al., 2001; Gao and Anderson, 2001). However, perturbations from human sources also exist, indicated by black carbon (BC) concentrations observed at this site (Tang et al., 1999).

Given the rare researches and data on aerosol chemical compositions in the QTP, more observational data are needed to better characterize the chemical composition of aerosols in the QTP. WSIs comprise a large portion of aerosol particles and may help understand chemical reactions in the atmosphere (Tripathee et al., 2017). They can provide important information for understanding chemical characterizations, sources, behaviors, and formation mechanisms; and hence, knowledge on the emission of gaseous precursors and the effect of regional and local pollution on ecosystem health (Wang et al., 2005; Tripathee et al., 2016). Furthermore, WSIs regulate the electrical properties of the atmospheric medium, participate in ion-catalyzed and ion–molecule reactions, and contribute to physicochemical interactions, including ion-induced new particle formation (Frege et al., 2017; Schulte and Arnold, 1990).

In this study, a real time monitor for WSIs associated with $PM_{2.5}$ was deployed at a national background monitoring site (Menyuan, Qinghai, 37º36'30"N, 101º15'26"E; 3295 m a.s.l.) in the northeastern QTP, following Du et al. (2015). Hourly mass concentrations of $PM_{2.5}$ bound sulfate, nitrate, ammonium, sodium, potassium, magnesium, and calcium were obtained during the 1^{st} –15^{th} October 2013. Real time measurements of SO_2, NO_X, CO, O_3, $PM_{2.5}$, and meteorological parameters were also recorded. We discuss the characterization and variation of WSIs; analyze the potential formation mechanisms of particulate SO_4^{2-} and NO_3^-, and investigate potential aerosol sources by combining WSI and gas pollutant data.

2. Methods

2.1 Monitoring site

Figure 1 shows the location of the monitoring site at the peak of Daban Mountain, Menyuan Hui Autonomous County, Qinghai Province (37º36'30"N, 101º15'26"E; 3295 m a.s.l.). The site is owned by the Chinese national atmospheric background monitoring station system and is approximately 160 km north of Xining, the capital city of Qinghai Province. The area is characterized by a typical plateau continental climate with an annual temperature of 0.8 ºC and precipitation of 520 mm. Meteorological parameters during the observation period are summarized in Table 1. The site is surrounded by typical QTP vegetation, including potentilla fruticosa and

Atmos. Chem. Phys. Discuss., https://doi.org/10.5194/acp-2018-1345
Manuscript under review for journal Atmos. Chem. Phys.
Discussion started: 23 January 2019

Atmospheric Chemistry and Physics Discussions

kobresia. No strong anthropogenic emission sources exist in the adjacent area, with the exception of occasional biomass burning events and yak dung burning for residential cooking and heating. The traffic volume around the site is small (Du et al., 2015).

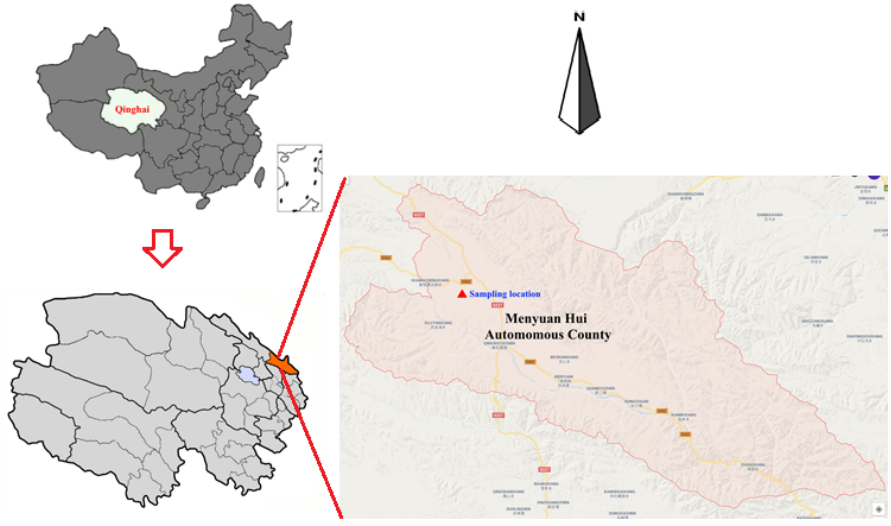

Figure 1 Location of sampling site

2.2 Instruments

Hourly concentrations of NO_3^-, SO_4^{2-}, Na^+, NH_4^+, K^+, Mg^{2+}, and Ca^{2+} associated with $PM_{2.5}$ were simultaneously measured by an ambient ion monitor (Model URG 9000B, URG Corporation, USA). A set of commercial instruments from Teledyne API (USA) were equipped to measure hourly concentrations of SO_2 (M100EU), $NO/NO_2/NO_x$ (M200EU), CO (M300EU), and O_3 (M400E). Hourly $PM_{2.5}$ concentrations were measured using an Ambient Dust Monitor 365 (GRIMM; Grimm Aerosol Technik GmbH &Co. KG, Ainring, Germany). Meteorological parameters (e.g. temperature, relative humidity, pressure, and wind speed and direction) were also recorded.

2.3 data analysis

2.3.1 Oxidant ratio

Particulate sulfate and nitrate oxidation ratios (SOR and NOR, respectively), defined as the molar ratio of SO_4^{2-} and NO_3^- to total oxidized sulfur and nitrogen (Zhou et al., 2009), were used to evaluate secondary conversion from NO_2 and SO_2 to NO_3^- and SO_4^{2-}, respectively. High SOR and NOR indicate larger conversions of SO_2 and NO_x to their respective particulate forms in $PM_{2.5}$. In this study, NOR and SOR were calculated based on the following formulae:

$$SOR = \frac{[SO_4^{2-}]}{[SO_2]+[SO_4^{2-}]} \quad (1)$$

Atmos. Chem. Phys. Discuss., https://doi.org/10.5194/acp-2018-1345
Manuscript under review for journal Atmos. Chem. Phys.
Discussion started: 23 January 2019

Atmospheric Chemistry and Physics Discussions

$$NOR = \frac{[NO_3^-]}{[NO_2]+[NO_3^-]} \quad (2)$$

2.3.2 Ion balance

Ion balance was used to evaluate the acid-base balance of aerosol particles. We converted the WSIs mass concentration into an equivalent concentration, as follows:

$$C\ (cation, \mu eq/m^3) = \frac{Na^+}{23} + \frac{NH_4^+}{18} + \frac{K^+}{39} + \frac{Mg^{2+}}{12} + \frac{Ca^{2+}}{20} \quad (3)$$

$$A\ (anion, \mu eq/m^3) = \frac{SO_4^{2-}}{48} + \frac{NO_3^-}{62} \quad (4)$$

2.3.3 Source apportionment

Positive Matrix Factorization (PMF), developed by Paatero (Paatero and Tapper, 1994; Paatero, 1997), has been widely applied in source apportionment researches. In this model, a data matrix X_{ij}, in which i is the sample and j is the measured chemical species, can be viewed as a speciated data set, and the concept of this model can be represented as:

$$X_{ij} = \sum_{k=1}^{p} g_{ik} f_{kj} + e_{ij} \quad (5)$$

where p is the number of factors; f is the chemical profile of each source, g is the mass contribution of each factor to the sample; f_{jk} is the source profile, and e_{ij} is the residual for each species or sample.

PMF solves Eq (5) by minimizing the sum of the square of residuals weighted inversely with the error estimates of the data points, Q, defined as:

$$Q = \sum_{i=1}^{n} \sum_{j=1}^{m} \left[\frac{x_{ij} - \sum_{k=1}^{p} g_{ik} f_{kj}}{u_{ij}} \right]^2 \quad (6)$$

where u_{ij} is the uncertainty of chemical species j in sample i.

Uncertainty for each species can be calculated using following equation:

$$Unc = \sqrt{(Error\ Fraction \times concentration)^2 + (MDL)^2} \quad (7)$$

where MDL is the method detective limit of each species.

Given that PMF is a descriptive model, there are no objective criteria for choosing the appropriate number of factors (Paatero et al., 2002). Therefore, several criteria were applied, including extracting realistic source profiles, distribution of scaled residuals, Q/Qexp, and the comparison between the PMF modeled and measured elemental mass (Crilley et al., 2017). In this study, the Q/Q_{exp} index was monitored with an increasing number of factors (3–6), because a large decrease is indicative of increased explanatory power, while a small decrease is suggestive of little improvement with additional factors. Consequently, the number of factors was chosen after Q/Q_{exp} decreased significantly. Q_{exp} was then calculated using the following equation:

$$Q_{exp} = N_{sample} \times M_{good} + \frac{N_{sample} \times M_{weak}}{3} - (N_{sample} \times P_{factor}) \quad (8)$$

Atmos. Chem. Phys. Discuss., https://doi.org/10.5194/acp-2018-1345
Manuscript under review for journal Atmos. Chem. Phys.
Discussion started: 23 January 2019

where N_{sample} is the number of samples in the model; M_{good} and M_{weak} are the number of good or weak model species, respectively; and P_{factor} is the number of estimated factors.

An argument on the application of PMF in this study is that the number of components associated with $PM_{2.5}$ is limited; therefore, more available data should be introduced into the model to ensure better source information and model results (Hopke, 2010). In previous studies, a practical way to extract more source information from the available data was to include data of other air pollutants such as volatile organic compounds (VOCs) (Wu et al., 2007a; Mo et al., 2017), major gaseous pollutants (NO_x, SO_2, and CO) (Rizzo and Scheff, 2007; Masiol et al., 2017), particle size distribution data (Zhou et al., 2005), and air trajectory and meteorological data (Buzcu-Guven et al., 2007). In this study, we introduced gaseous pollutants data, combined them with WSIs data, and applied the new dataset into the PMF model.

2.3.4 Statistical analysis

Correlation analysis, analysis of variation (ANOVA), and linear regression were applied. All statistical calculations were preformed using R studio software packages (Version 0.99.903, RStudio, Inc.).

3. Results and Discussion

3.1 Descriptive analysis

Table 1 summarizes the concentrations of WSIs, $PM_{2.5}$, and gaseous pollutants and data of meteorological parameters during the observation period. SO_4^{2-} accounted for 67.9% of the total WSIs mass, followed by NH_4^+ (13.7%), and NO_3^- (11.2%). SO_4^{2-}, NO_3^- and NH_4^+ (SNA), accounting for 92.8% of the total WSIs mass, were the major components of secondary inorganic aerosols.

Atmos. Chem. Phys. Discuss., https://doi.org/10.5194/acp-2018-1345
Manuscript under review for journal Atmos. Chem. Phys.
Discussion started: 23 January 2019

Atmospheric Chemistry and Physics Discussions

212 Table 1 Descriptive statistics of WSIs species, gaseous pollutants and meteorological parameters

Species	Mean	Standard Deviation	Percentile				
			5th	25th	50th	75th	95th
WSIs (μg/m^3)							
NO_3^-	1.65	0.71	0.62	1.14	1.60	2.02	2.90
SO_4^{2-}	10.00	4.39	6.39	7.05	8.37	10.73	18.83
Na^+	0.86	0.61	0.01	0.50	0.79	1.12	1.66
NH_4^+	2.02	0.93	0.52	1.40	1.95	2.54	3.59
K^+	0.05	0.03	0.01	0.03	0.04	0.06	0.11
Mg^{2+}	0.06	0.19	0.01	0.02	0.04	0.05	0.09
Ca^{2+}	0.09	0.05	0.01	0.05	0.09	0.11	0.18
$[NO_3^-]/[SO_4^{2-}]$	0.29	0.13	0.11	0.19	0.29	0.37	0.49
Air pollutants (μg/m^3)							
$PM_{2.5}$	18.99	13.10	2.60	9.00	16.15	26.35	44.28
SO_2	4.37	5.76	1.28	1.79	2.40	3.88	14.70
NO	0.12	0.19	0.01	0.02	0.04	0.13	0.45
NO_2	4.35	2.66	1.42	2.58	3.96	5.26	8.99
NO_X	4.45	2.70	1.42	2.68	4.14	5.33	9.02
CO	48.59	56.51	4.60	13.65	26.31	58.35	183.57
O3	107.71	25.13	82.91	92.74	106.93	117.72	134.02
Acidity (μeq/m^3)							
Anion	0.22	0.11	0.01	0.17	0.19	0.26	0.42
Cation	0.13	0.08	0.00	0.05	0.14	0.17	0.25
Oxidation Ratio							
SOR	0.65	0.16	0.34	0.56	0.69	0.75	0.88
NOR	0.22	0.10	0.10	0.16	0.20	0.26	0.38
Meteorological Parameters							
Temp (°C)	6.55	4.53	0.50	2.80	5.60	10.70	14.49
RH (%)	52.92	18.44	22.56	38.40	55.80	65.80	81.56
Pressure (kPa)	68.58	0.26	68.10	68.30	68.60	68.80	68.90
Wind Speed (m/s)	3.39	3.02	0.00	1.30	2.60	4.70	9.20

213

214

Atmos. Chem. Phys. Discuss., https://doi.org/10.5194/acp-2018-1345
Manuscript under review for journal Atmos. Chem. Phys.
Discussion started: 23 January 2019

Atmospheric Chemistry and Physics Discussions

215 Table 2 Comparisons of WSIs concentrations with other high altitude and urban sites (mean, μg/m^3)

Sampling site	Sampling Year	SO_4^{2-}	NO_3^-	Na^+	NH_4^+	K^+	Ca^{2+}	Mg^{2+}	$[NO_3^-]/[SO_4^{2-}]$	Reference
The QTP site										
Menyuan, Qinghan, the northeastern QTP (3295m)	2013	10.0	1.6	0.9	2.09	0.05	0.09	0.06	0.29	This study
South edge of the QTP (4276m)	2009	0.43	0.20	0.07	0.03	0.02	0.88	0.04	0.72	Cong et al. (2015)
Qilian Shan Station, the northeastern QTP (4180m)	2010	0.74	0.20	0.04	0.15	0.04	0.18	0.04	0.42	Xu et al. (2014)
Qinghai Lake, the northeastern QTP (3200m)	2010	4.45	0.38	0.13	-	0.12	0.23	0.06	0.13	Zhang et al. (2014)
	2012	3.65	1.42	0.26	0.62	0.10	0.66	0.10	0.60	Zhao et al. (2015)
Low altitude site in China (urban and background sites)										
Sampling site	Sampling Year	SO_4^{2-}	NO_3^-	Na^+	NH_4^+	K^+	Ca^{2+}	Mg^{2+}	$[NO_3^-]/[SO_4^{2-}]$	Reference
Beijing (43m)	2013	13.80	15.43	0.69	8.02	1.06	0.08	0.58	1.28	Dao et al. (2014)
Shanghai (4m)	2009	12.9	15.0	-	6.64	0.94	-	-	1.80	Ming et al. (2017)
Xi'an (396m)	2006	42.0	20.6	-	13.1	-	-	-	0.76	Zhang et al. (2011)
Chongqing (160m)	2012	15.4	8.4	0.25	6.9	0.67	0.24	0.04	0.84	Chen et al. (2017)
Shangdianzi, Beijing (293m)	2009	8.68	11.20	-	3.23	-	-	-	2.00	Zhao et al. (2013a)
Lin'an, Zhejiang (138m)	2014	15.9	11.7	2.6	4.9	1.1	3.7	0.2	1.14	Zhang et al. (2017)
Other high-altitude area sites around the world										
Sampling site	Sampling Year	SO_4^{2-}	NO_3^-	Na^+	NH_4^+	K^+	Ca^{2+}	Mg^{2+}	$[NO_3^-]/[SO_4^{2-}]$	Reference
Langtang, remote Himalayas, Nepal (3920m)	1999-2000	0.27	0.04	0.06	0.15	0.02	0.03	0.004	0.23	(Carrico et al., 2003)
Nagarkot, Kathmandu Valley, Nepal (2150m)	1999-2000	2.5	0.8	0.13	1.2	0.28	0.05	0.01	0.50	(Carrico et al., 2003)
Gurushikhar in Mt. Abu, Indian (1680 m)	2007	3.56	-	0.28	0.92	0.10	0.19	0.06	-	(Kumar and Sarin, 2010)
Golden, Colorado, USA (1850 m)	2014	0.67	0.40	-	0.60	-	-	-	0.92	(Valerino et al., 2017)
Monte Martano, Italy (1100 m)	2009	1.90	0.84	0.02	0.54	0.06	0.25	0.06	0.68	(Moroni et al., 2015)
Lassen Volcanic National Park, California, USA (1798	2009-2012	0.35	0.12	-	-	-	0.04	-	0.53	(VanCuren and Gustin, 2015)

m) Great Basin National Park, Nevada, USA (2060 m)	2009-2012	0.38	0.10	-	-	-	0.05	-	0.41	(VanCuren and Gustin, 2015)

To better understand the concentrations of WSIs, we compared our observations with other studies implemented in background sites or urban sites across China and high altitude areas around the world in Table 2. Our results are lower as compared to studies in Europe and the USA (VanCuren and Gustin, 2015; Valerino et al., 2017; Moroni et al., 2015), and the high latitude Himalaya region (Carrico et al., 2003); however, observations are comparable with some urban area in India and Nepal (Carrico et al., 2003; Kumar and Sarin, 2010). Observed concentrations of SO_4^{2-} are also lower as compared to low altitude sites in China, for example urban sites in Beijing, Shanghai, Xi'an, and Chongqing and background sites in Shangdianzi (Beijing) and Lin'an (Zhejiang). Concentrations of NO_3^- were five to thirteen times lower as compared to those in low altitude areas (both urban and background sites), indicating that the influence of vehicle emissions in studying area is weak. NH_4^+ levels were lower as compared to those in urban sites (three to six times lower), and also slightly lower as compared to background sites (less than three times lower).

SNA concentrations in this study were higher as compared to those at other sites in the QTP, including the southern edge (Cong et al., 2015), Qilian Shan Station (Xu et al., 2014), and Qinghai Lake in the northeastern QTP (Zhang et al., 2014; Zhao et al., 2015). Large differences in concentrations suggest that the monitoring site in this study appears to be more impacted by natural and human activities as compared to other sites in the QTP.

Tables 1 and 2 show the molar ratios of NO_3^- and SO_4^{2-}, an indicator of the relative importance of vehicle versus coal combustion emissions in the atmosphere (Arimoto et al., 1996; Yao et al., 2002). The ratio in this study (0.29±0.13) is lower as compared to low altitude areas, which are characterized as vehicle emission dominant or co-dominant by vehicle and coal emissions. The ratio varies apparently across the different sites in the QTP as shown in Table 2. Even at a single monitoring site (Qinghai Lake; Table 2), different studies reported different ratios (Zhang et al., 2014; Zhao et al., 2015). Thus, it is likely that remote transportation and local emissions jointly affect air pollution over these monitoring sites.

Atmos. Chem. Phys. Discuss., https://doi.org/10.5194/acp-2018-1345
Manuscript under review for journal Atmos. Chem. Phys.
Discussion started: 23 January 2019

Atmospheric Chemistry and Physics Discussions

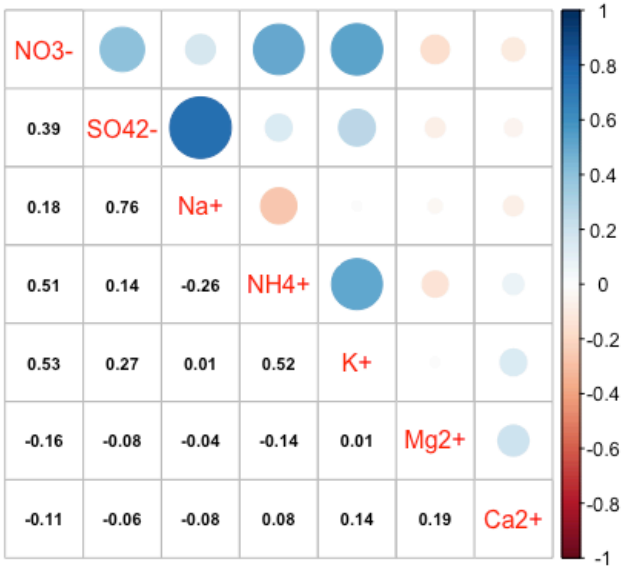

Figure 2 Correlation coefficients (r) between WSIs in $PM_{2.5}$ during sampling period

Correlations between WSIs are useful to investigate potential associations between the various WSIs (Xu et al., 2014). Figure 2 illustrates the correlation coefficients between WSIs based on their mass concentrations. A high correlation was found between Na^+ and SO_4^{2-} (r=0.76). NO_3^- and SO_4^{2-} had a negative and weak correlation with Mg^{2+} and Ca^{2+}, which were found to be highly correlated with CO_3^{2-} in another study in the QTP (Xu et al., 2014). SNA displayed medium positive correlations with each other. K^+, commonly used as a marker for emissions from the burning of biomass or biofuel, had a medium correlation with NH_4^+ and NO_3^-.

To further examine the relationship between $PM_{2.5}$ and WSIs, we divided the $PM_{2.5}$ concentrations into four categories: a) $C(PM_{2.5}) < 20\mu g/m^3$, (b) $20\mu g/m^3 \leq C(PM_{2.5}) < 30\mu g/m^3$, (c) $30\mu g/m^3 \leq C(PM_{2.5}) < 40\mu g/m^3$, and (d) $C(PM_{2.5}) \geq 40\mu g/m^3$ and attributed each WSI measurement to its corresponding $PM_{2.5}$ category. Figure 3 shows the mean proportions of WSIs in $PM_{2.5}$ for the different categories. As the $PM_{2.5}$ concentration increases, the percentages of WSIs in $PM_{2.5}$ mass exhibited decreasing trends, suggesting that the contribution of WSIs to $PM_{2.5}$ increases was negligible. Du et al. (2015) deployed an Aerodyne Aerosol Chemical Speciation Monitor simultaneously with our study, and found that organics were the only species that increased during the particle growth period. This finding suggests that organics, rather than WSIs, are playing a dominant role in particle growth at the national background site, rather than ammonium sulfate. Other studies have also confirmed this finding (Dusek et al., 2010; Ehn et al., 2014; Setyan et al., 2014).

Atmos. Chem. Phys. Discuss., https://doi.org/10.5194/acp-2018-1345
Manuscript under review for journal Atmos. Chem. Phys.
Discussion started: 23 January 2019

Atmospheric Chemistry and Physics Discussions

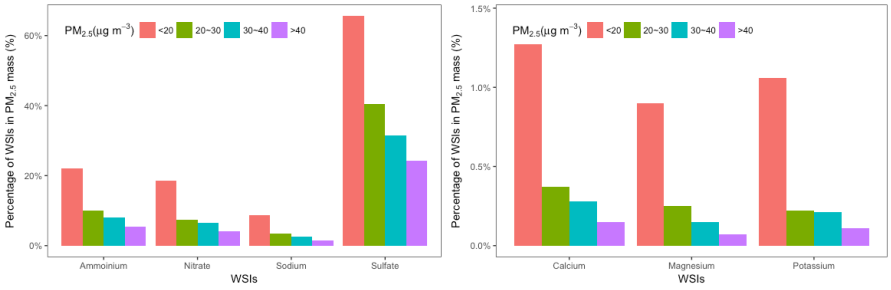

Figure 3 Mass portions of WSIs within different $PM_{2.5}$ level ranges

3.2 Diurnal variation analysis

Diurnal variations of WSIs in $PM_{2.5}$, related gaseous pollutants (SO_2, NO_2, and O_3), and meteorological parameters (temperature, relative humidity, and wind speed) are shown in Figure 4.

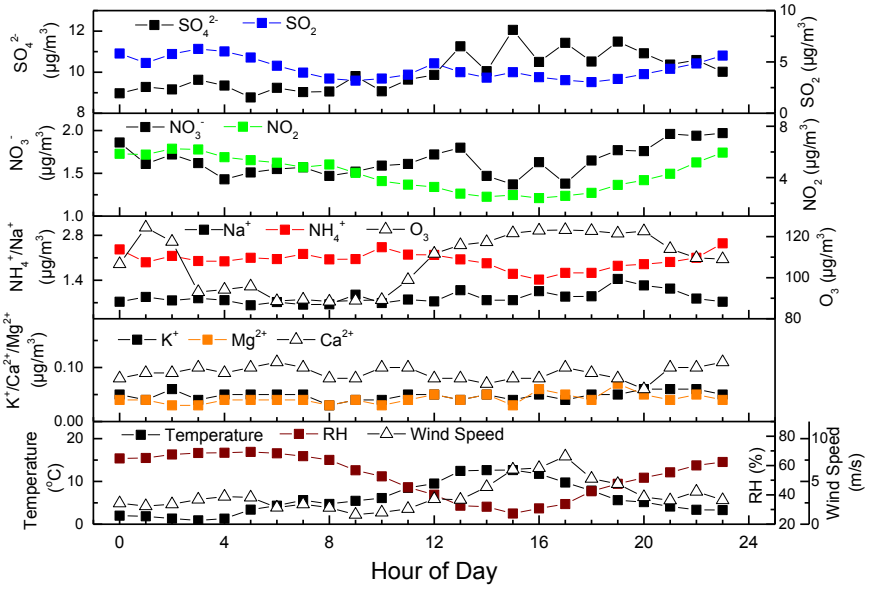

Figure 4 Diurnal variations of WSIs in $PM_{2.5}$, gaseous pollutants (SO_2, NO_2, O_3), as well as meteorological parameters (temperature, relative humidity and wind speed) during sampling period

SO_4^{2-} concentrations begin to increase from midnight (Beijing time), reach peak levels at approximately 15:00, and then decrease gradually. SO_2 concentrations exhibit a bimodal trend, with peaks at 03:00 and 12:00; conversely, SO_4^{2-} exhibits an inverse trend. NO_3^- concentrations peak at midnight and in the early afternoon, with lowest levels occurring during the late afternoon. NO_2 displays high nighttime levels and low daytime levels. NH_4^+ remains steady during the morning with a peak at 10:00. O_3, temperature, RH, and wind speed also display evident diurnal variations; O_3, temperature, and wind speed are low (high) at night (day), while RH shows an inverse

Atmos. Chem. Phys. Discuss., https://doi.org/10.5194/acp-2018-1345
Manuscript under review for journal Atmos. Chem. Phys.
Discussion started: 23 January 2019

Atmospheric Chemistry and Physics Discussions

variation to this pattern.

3.3 Sulfate and nitrate oxidation ratio analysis

Average NOR and SOR during the whole measurement campaign were 0.22 and 0.65, respectively, suggesting potentially strong secondary formation of both SO_4^{2-} and NO_3^-. Strong photochemical reactions and the existence of high O_3 concentrations would elevate the oxidant ratio from SO_2 and NO_2 to SO_4^{2-} and NO_3^-, despite the low intensity of local emissions. Furthermore, remote transportation also contributed to the concentrations of SO_4^{2-} and NO_3^-, thus increasing the oxidant ratio, despite not being products of local oxidation.

Variation trends of SOR and NOR were compared to changes in $PM_{2.5}$ concentration and ambient RH, as shown in Figure 5. Previous research has shown that, in urban areas, both SOR and NOR increased with the $PM_{2.5}$ concentration, suggesting that heavy $PM_{2.5}$ pollution corresponds to high SOR and NOR (Xu et al., 2017). However, studies investigating SOR and NOR variations at background sites with low $PM_{2.5}$ concentration range are rare. Our results showed that increasing concentrations of $PM_{2.5}$ at low levels corresponded to decreasing SOR and NOR (Figure 5a), although the decreases were slight. This is consistent with our previous finding that concentrations of SO_4^{2-} and NO_3^- did not vary markedly with $PM_{2.5}$ increases at background sites, and provides further evidence to suggest that SO_4^{2-} and NO_3^- are not key drivers of $PM_{2.5}$ growth at low levels. The simultaneous observations of Du et al. (2015), indicated that organics were thought to be the major driver of particle growth.

In Figure 5b, SOR initially decreases and then increases as RH increases. Peak SOR occurs when RH reaches both its maximum and minimum levels, when RH is low (10–20%), O_3 is high (114.6 μg/m^3, approximately the 70th percentile of O_3 concentrations), and vice versa (RH > 70% and O_3 93.8 μg/m^3, approximately the 30th percentile of O_3 concentrations). The formation of particulate SO_4^{2-} can be achieved via aqueous-phase oxidation (heterogeneous reaction) or gas-phase oxidation (photochemical reaction). Normally, aqueous-phase oxidation from SO_2 to SO_4^{2-} is faster than gas-phase oxidation (Wang et al., 2016). When RH is low and O_3 is high, the photochemical formation of SO_4^{2-} via gas-phase oxidation should be considered the main oxidation pathway. Conversely, low O_3 and high RH are not sufficient to provide adequate oxidizing capacity; thus photochemical SO_4^{2-} formation becomes less important and aqueous-phase oxidation plays a more dominant role.

NOR constantly decreases as RH increases. Particulate NO_3^- is predominantly formed by the gas-phase reaction of NO_2 and OH radicals during the day and by heterogeneous reactions of nitrate radicals (NO_3) at night (Seinfeld and Pandis, 2016). In this study, high (low) O_3 and low (high) RH lead to high (low) NOR, meaning that gas-phase reactions oxidized by high levels of O_3 are the major pathway for nitrate formation, while heterogeneous reactions play a less important role.

Trends of SOR and NOR with RH and O_3 suggest that both photochemical and heterogeneous reactions contribute to the secondary transformation of SO_2, while only photochemical reaction drives the conversion of NO_2 to nitrate.

Atmos. Chem. Phys. Discuss., https://doi.org/10.5194/acp-2018-1345
Manuscript under review for journal Atmos. Chem. Phys.
Discussion started: 23 January 2019

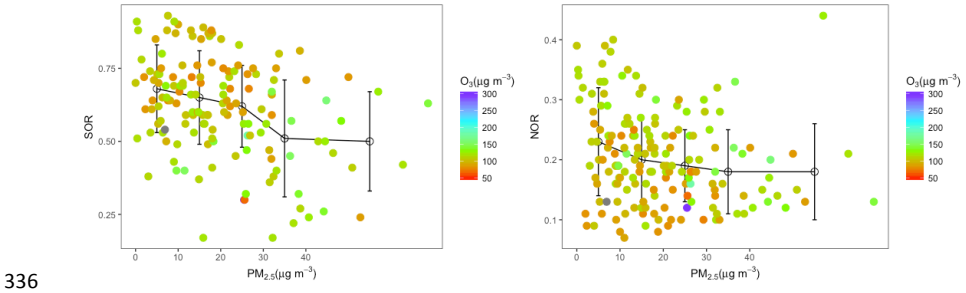

(a) $PM_{2.5}$

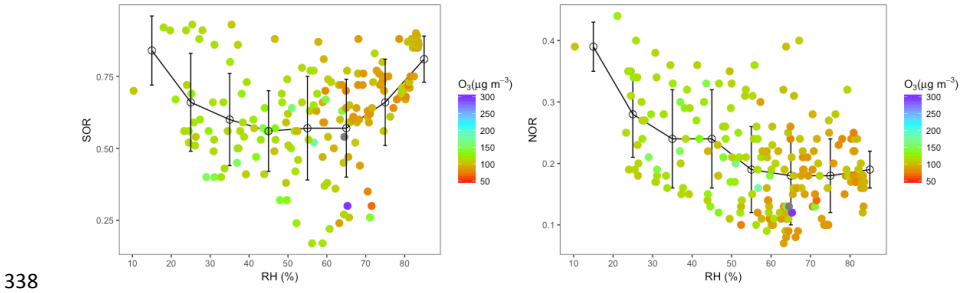

(b) RH

Figure 5 Variations of SOR and NOR as a function of $PM_{2.5}$ and RH. The vertical bars correspond to one standard error from the mean.

Figure 6 characterizes the diurnal variations of SO_4^{2-}, NO_3^-, SOR, NOR, O_3, and RH. The variation of SOR is small, particularly as compared to the evident diurnal variation in SO_4^{2-}. Daytime gas-phase oxidation and nighttime aqueous-phase oxidation are thought to be equally important to the formation of SO_4^{2-}. NOR is high during the day and low at night; reflecting a strong positive correlation with O_3 ($r=0.71$, $p<0.05$) and a weak negative correlation with RH ($r=-0.43$, $p<0.05$). The high correlation between NOR and O_3 indicates that gas-phase oxidation via photochemical reactions is the main NO_3^- formation pathway.

It is apparent that photochemical reactions (dominated by O_3 oxidization) contribute markedly to the secondary conversion of both SO_2 and NO_2, while heterogeneous reactions (promoted by the existence of aqueous phase) contributed to the formation of SO_4^{2-} and only had a weak effect on NO_3^-. Ma et al. (2003) found that fine nitrate particles (Dp < 2.0 μm) at Waliguan Observatory (150 km south of our monitoring site) were most likely produced via gaseous-phase reactions between nitric acid and ammonia, in line with our findings on nitrate formation.

Atmos. Chem. Phys. Discuss., https://doi.org/10.5194/acp-2018-1345
Manuscript under review for journal Atmos. Chem. Phys.
Discussion started: 23 January 2019

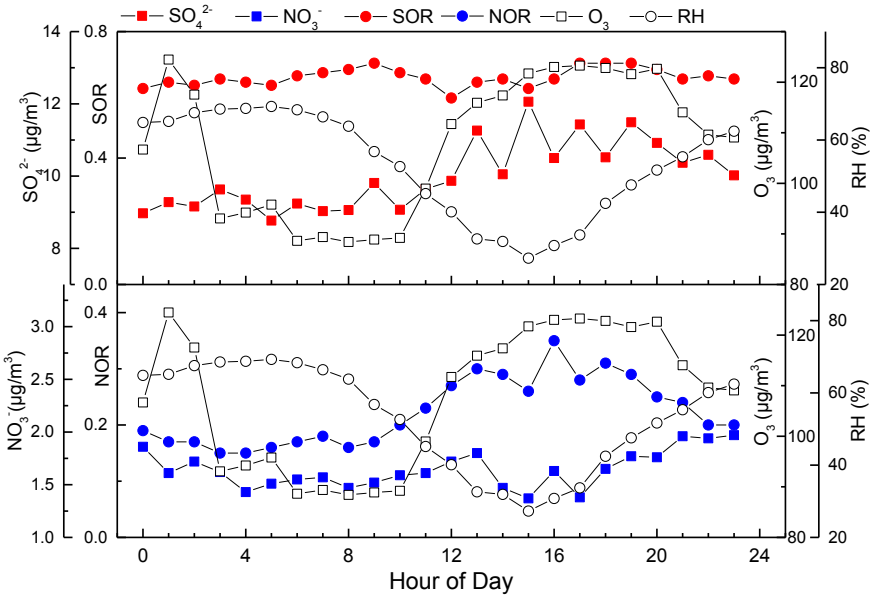

Figure 6 Diurnal variations of SO_4^{2-} and NO_3^-, SOR, NOR O_3 and RH during sampling period

3.4 Molecular composition of major ionic species

The molecular chemical forms of the major WSIs in $PM_{2.5}$ were identified using bivariate correlations based on individual WSI molar concentrations (Verma et al., 2010; Wang et al., 2005). In this study, we used equivalent concentrations for correlation analysis, and the coefficients are shown in Table 3. Figure 7 a–c show scatter plots of the equivalent concentrations of $[NH_4^+]$ and $[NO_3^-]$, $[Na^+]$ and $[SO_4^{2-}]$, and $[NH_4^+]$ and $[SO_4^{2-} + NO_3^-]$, respectively. $(NH_4)_2SO_4$ and NH_4NO_3 are major components of atmospheric aerosols (Park et al., 2004), commonly formed by the neutralization of sulfuric acid (H_2SO_4) and nitric acid (HNO_3) by NH_3 (Xu et al., 2014). It is apparent that NH_4^+ is closely correlated with NO_3^- (r=0.56). The slope of the regression between NH_4^+ and NO_3^- (μep/m^3 versus μep/m^3) is 2.28, indicating the complete neutralization of NO_3^- by NH_4^+. SO_4^{2-} was highly correlated with Na^+ (r=0.56), rather than NH_4^+. Unlike NO_3^- and NH_4^+, Na^+ was completely neutralized by SO_4^{2-} (slope=0.15) in the form of $NaHSO_4$. Excess NH_4^+ would then combine with excess SO_4^{2-} (r=0.46). The regression slope between excess NH_4^+ and excess SO_4^{2-} was 0.72, meaning that excess NH_4^+ was completely neutralized by SO_4^{2-} and existed in the form of $(NH_4)_2SO_4$. Excess sulfuric acid was likely neutralized by crustal WSIs; and K_2SO_4 was a major chemical species in aerosol particles based on their correlation coefficients. Good regression results between $[NH_4^+ + Na^+ + K^+]$ and $[NO_3^- + SO_4^{2-}]$ were also observed in Figure 7 d.

Atmos. Chem. Phys. Discuss., https://doi.org/10.5194/acp-2018-1345
Manuscript under review for journal Atmos. Chem. Phys.
Discussion started: 23 January 2019

Table 3 Correlation coefficients (r) between the equivalent concentrations of WSIs in $PM_{2.5}$ during sampling period

	NO_3^-	SO_4^{2-}	Na^+	NH_4^+	K^+	Mg^{2+}	Ca^{2+}
NO_3^-							
SO_4^{2-}	0.49						
Na^+	0.17	0.56					
NH_4^+	0.56	0.46	-0.24				
K^+	0.56	0.39	0.06	0.57			
Mg^{2+}	-0.11	-0.13	-0.06	-0.15	-0.03		
Ca^{2+}	-0.06	-0.11	0.01	-0.08	0.03	0.09	

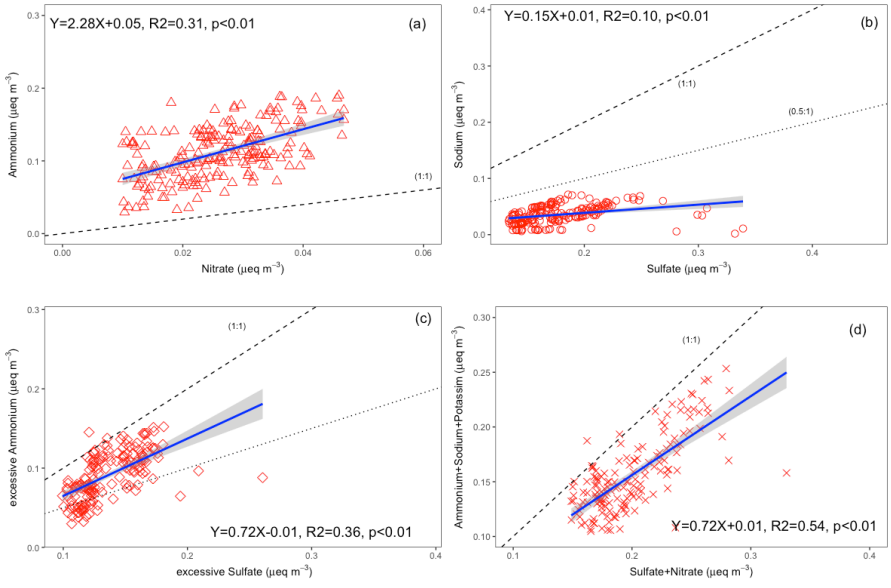

Figure 7 Scatter plot of (a) [NH_4^+] and [NO_3^-] (b) [Na^+] and [SO_4^{2-}] (c) [excessive NH_4^+] and [excessive SO_4^{2-}] (d) [$NH_4^+ + Na^+ + K^+$] and [$NO_3^- + SO_4^{2-}$]

3.5 Ion acidity analysis

The ion balance, expressed by the sum of the equivalent concentration (μeq/m^3) ratio of cation to anion (C/A), is an indicator of the acidity of particulate matter (Wang et al., 2005). In this study, the ion balance ratio was 0.87, indicating that aerosols tended to be acid, in line with previous studies in the QTP (Xu et al., 2015; Zhao et al., 2015). This suggests that anthropogenic emissions (e.g. SO_4^{2-} and NO_3^-), either regional or local, impacted aerosol acidity during the observation period, and that the contribution from mineral dust was weak.

Figure 8 shows the scatter and linear regression plot of cations and anions (μeq/m^3). It is apparent that most points are below the 1:1 line, highlighting the acid

Atmos. Chem. Phys. Discuss., https://doi.org/10.5194/acp-2018-1345
Manuscript under review for journal Atmos. Chem. Phys.
Discussion started: 23 January 2019

Atmospheric Chemistry and Physics Discussions

tendency. The total equivalent anion concentration was regressed against the total equivalent concentrations of cations, and the slope of regression was 0.58.

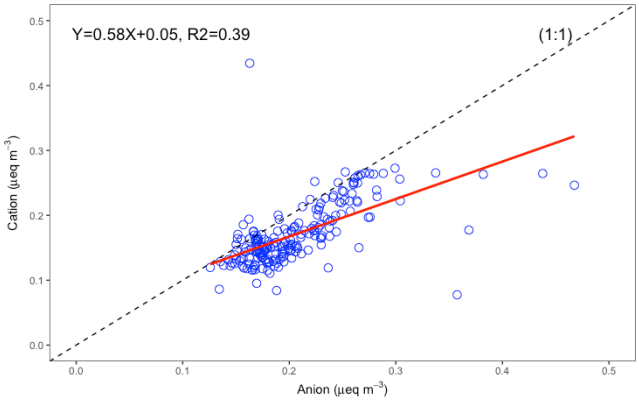

Figure 8 Cation and Anion scatter plot and linear regression

Aerosol acidity for different categories of $PM_{2.5}$ concentration (described in section 3.1) and their respective scatter plots of total equivalent concentrations of anions and cations are shown in Figure 9. C/A was high when $PM_{2.5}$ concentrations exceeded 20μg/m^3, indicating that aerosol acidity was weak when the $PM_{2.5}$ concentration was high. This provides further evidence to support our finding that SO_4^{2-} and NO_3^- did not contribute to $PM_{2.5}$ increases.

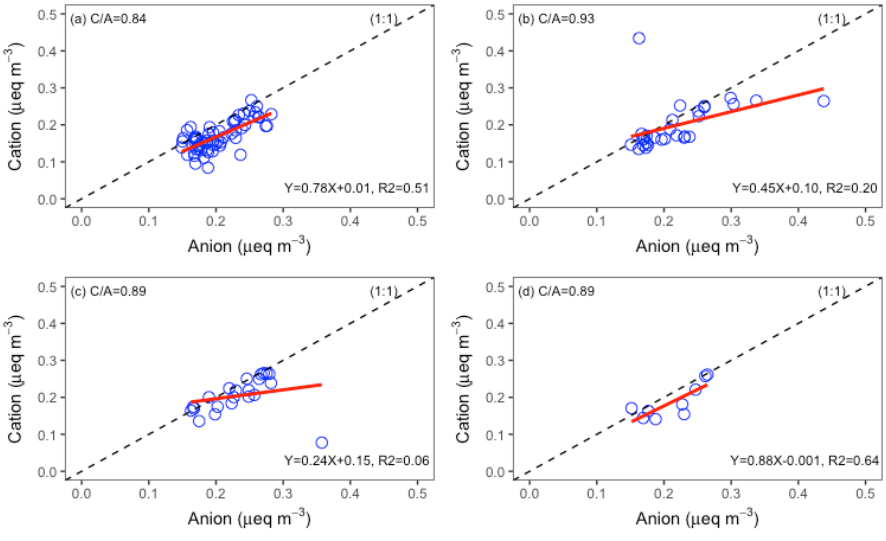

Figure 9 Scatter plot Σ Anion and Σ Cation with different $PM_{2.5}$ concentration range (a) C($PM_{2.5}$) < 20μg/m^3 (b) 20μg/m^3 ≤ C($PM_{2.5}$) <30μg/m^3 (c) 30μg/m^3 ≤ C($PM_{2.5}$) <40μg/m^3 (d) C($PM_{2.5}$) ≥ 40μg/m^3

Atmos. Chem. Phys. Discuss., https://doi.org/10.5194/acp-2018-1345
Manuscript under review for journal Atmos. Chem. Phys.
Discussion started: 23 January 2019

Atmospheric Chemistry and Physics Discussions

3.6 Source apportionment by PMF

In this study, all WSIs and gaseous pollutants were introduced into the PMF model for source identification. We ran the PMF model with different numbers of factors to determine the Q/Q_{exp} variation. The Q/Q_{exp} decrease between four and five factors was the largest (Figure 10); therefore, five factors were used in the PMF model. The distributions of the factor species and the percentage of total species are shown in Figure 11.

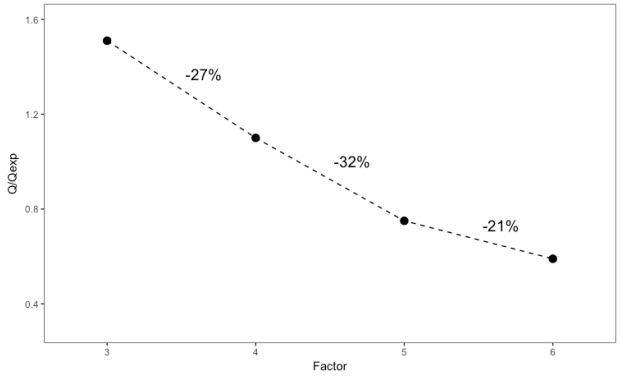

Figure 10 The decrease ratio of Q/Q_{exp} with different number of factor choice

Atmos. Chem. Phys. Discuss., https://doi.org/10.5194/acp-2018-1345
Manuscript under review for journal Atmos. Chem. Phys.
Discussion started: 23 January 2019

Atmospheric Chemistry and Physics Discussions

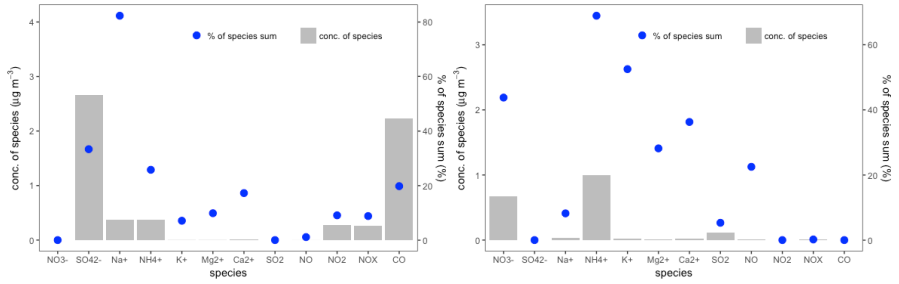

(a) (b)

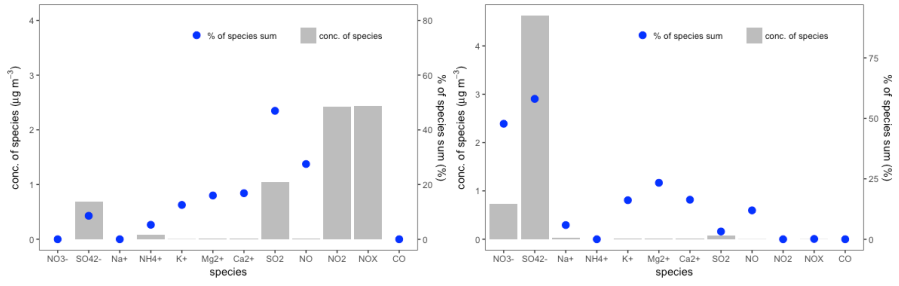

(c) (d)

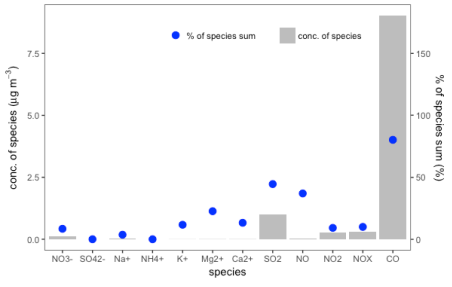

(e)

Figure 11 Source profiles exacted by PMF (a) Factor 1: salt lake emissions; (b) Factor 2: Crustal dust, animal waste emission and biomass burning; (c) Factor 3: Vehicle emissions; (d) Factor 4: Secondary inorganic aerosol; (e) Domestic burning (black circle represented the percentage of species sum, while white bar represented concentration of species)

Factor 1 has high Na^+ loading and a moderate SO_4^{2-} loading. Our monitoring site is approximately 100 km from Qinghai Lake, a saline and alkaline water body which is the largest lake in China. Zhang et al. (2014) collected total suspended particle (TSP) and $PM_{2.5}$ samples at Qinghai Lake, and found that the concentration of Na^+ was higher as compared to other mountainous areas. Furthermore, they found that SO_4^{2-} was one the most abundant species in both TSP and $PM_{2.5}$. Therefore, we attribute factor 1 to aerosols emitted from Qinghai Lake.

High NH_4^+ and K^+ loading and moderate Mg^{2+} and Ca^{2+} loading were observed in factor 2. Livestock feces, which is commonly found in the meadows around the

sampling site is a possible source of NH_4^+. K^+ can be attributed to the combustion of biomass, which has both natural and anthropogenic origins. Li et al. (2015) found that occasional biomass burning events in the area contributed significantly to the formation of anthropogenic fine particles. Moreover, crustal materials were considered as major sources of Mg^{2+} and Ca^{2+} (Ma et al., 2003). Consequently, factor 2 is attributed to mixed sources, including livestock waste emissions, biomass burning, and crustal materials.

Factor 3 is identified as traffic emissions due to high contributions of NO_2 and NO_x, and a moderate SO_2 loading. A national road (G227) and a provincial road (S302) pass near the monitoring site, and many of the transient vehicles are heavy-duty trucks. Consequently, road emissions do influence the monitoring site, irrespective of the low traffic volume.

Factor 4 is secondary inorganic aerosol, enriched with SO_4^{2-} and NO_3^-. The precursor of SO_4^{2-} is SO_2, which may originate from coal combustion, and NO_3^- is mainly converted from ambient NO_x, emitted by both vehicle exhaust and fossil fuel combustion.

Factor 5 has a CO high loading and moderate SO_2 and NO loading. Residential cooking and heating often causes heavy indoor air pollution, especially elevated of CO (Naeher et al., 2000). Yak dung is the primary energy source for cooking and heating by nomadic Tibetan herders (Li et al., 2012). Thus, factor 5 is attributed to the burning of yak dung for residential heating and cooking.

4. Conclusion

The QTP is an ideal location for characterizing aerosol properties. In this study, we investigated the characterizations of WSIs associated with autumn $PM_{2.5}$ at a background site (3295 m a.s.l.) in the QTP. Real time levels of WSIs, $PM_{2.5}$, gaseous pollutants, and meteorological parameters were collected to analyze the ion chemistry of aerosols in the QTP. SO_4^{2-}, NO_3^-, and NH_4^+ (SNA) were the three most abundant WSI species, and crust-originated ions (Na^+, Mg^{2+}, K^+, and Ca^{2+}) comprised a small fraction of total WSIs. As compared to similar studies in China, SNA concentrations in this study were lower as compared to low altitude urban areas, but higher relative to other sites in the QTP.

Further investigation regarding the formation of SO_4^{2-} and NO_3^- revealed that strong solar intensity and high O_3 concentrations combined with low daytime RH greatly enhanced the conversion of SO_2 and NO_2 to SO_4^{2-} and NO_3^-, respectively. Heterogeneous reactions were weak overnight, and contributed to SO_4^{2-} formation only. Our analysis suggests that photochemical reactions played a critical role in the formation of SO_4^{2-} and NO_3^- during our observation period.

Source apportionment using a PMF model identified five factors: salt lake emissions, mixed factor emissions (livestock feces, biomass burning, and crustal material emissions), traffic emissions, secondary inorganic aerosols, and residential burning. With the exception of some natural sources (salt lake, livestock and crustal materials), anthropogenic emissions demonstrated a marked contribution to

particulate loading in the area. For example, traffic emissions near the site, although limited, still influenced local air quality. Hence, greater controls should be imposed on diesel quality and heavy-duty truck emissions in this area to minimize traffic pollution.

Data Availability

All data of this work can be obtained from Bin Han (hanbin@craes.org.cn)

Author Contributions

BH, WY and ZB designed the experiments. BY, XW and XD were in charge of the whole field experiment. JW and XZ processed the original data and primary analysis. BH prepared the manuscript with contributions from all co-authors

Reference

Arimoto, R., Duce, R. A., Savoie, D. L., Prospero, J. M., Talbot, R., Cullen, J. D., Tomza, U., Lewis, N. F., and Jay, B. J.: Relationships among aerosol constituents from Asia and the North Pacific during PEM-West A, J. Geophys. Res.-Atmos., 101, 2011-2023, 10.1029/95jd01071, 1996.

Buzcu-Guven, B., Brown, S. G., Frankel, A., Hafner, H. R., and Roberts, P. T.: Analysis and apportionment of organic carbon and fine particulate matter sources at multiple sites in the Midwestern United States, Journal of the Air & Waste Management Association, 57, 606-619, 10.3155/1047-3289.57.5.606, 2007.

Cao, J. J., Lee, S. C., Chow, J. C., Watson, J. G., Ho, K. F., Zhang, R. J., Jin, Z. D., Shen, Z. X., Chen, G. C., Kang, Y. M., Zou, S. C., Zhang, L. Z., Qi, S. H., Dai, M. H., Cheng, Y., and Hu, K.: Spatial and seasonal distributions of carbonaceous aerosols over China, J. Geophys. Res.-Atmos., 112, 10.1029/2006jd008205, 2007.

Carrico, C. M., Bergin, M. H., Shrestha, A. B., Dibb, J. E., Gomes, L., and Harris, J. M.: The importance of carbon and mineral dust to seasonal aerosol properties in the Nepal Himalaya, Atmos. Environ., 37, 2811-2824, https://doi.org/10.1016/S1352-2310(03)00197-3, 2003.

Chen, Y., Xie, S.-d., Luo, B., and Zhai, C.-z.: Particulate pollution in urban Chongqing of southwest China: Historical trends of variation, chemical characteristics and source apportionment, Science of The Total Environment, 584–585, 523-534, https://doi.org/10.1016/j.scitotenv.2017.01.060, 2017.

Cong, Z., Kang, S., Kawamura, K., Liu, B., Wan, X., Wang, Z., Gao, S., and Fu, P.: Carbonaceous aerosols on the south edge of the Tibetan Plateau: concentrations, seasonality and sources, Atmos. Chem. Phys., 15, 1573-1584, 10.5194/acp-15-1573-2015, 2015.

Crilley, L. R., Lucarelli, F., Bloss, W. J., Harrison, R. M., Beddows, D. C., Calzolai, G., Nava, S., Valli, G., Bernardoni, V., and Vecchi, R.: Source apportionment of fine and coarse particles at a roadside and urban background site in

London during the 2012 summer ClearfLo campaign, Environ. Pollut., 220, Part B, 766-778, http://dx.doi.org/10.1016/j.envpol.2016.06.002, 2017.

Dao, X., Wang, Z., Lv, Y., Teng, E., Zhang, L., and Wang, C.: Chemical Characteristics of Water-Soluble Ions in Particulate Matter in Three Metropolitan Areas in the North China Plain, PLOS ONE, 9, e113831, 10.1371/journal.pone.0113831, 2014.

Du, W., Sun, Y. L., Xu, Y. S., Jiang, Q., Wang, Q. Q., Yang, W., Wang, F., Bai, Z. P., Zhao, X. D., and Yang, Y. C.: Chemical characterization of submicron aerosol and particle growth events at a national background site (3295 m a.s.l.) on the Tibetan Plateau, Atmos. Chem. Phys., 15, 10811-10824, 10.5194/acp-15-10811-2015, 2015.

Dusek, U., Frank, G. P., Curtius, J., Drewnick, F., Schneider, J., Kurten, A., Rose, D., Andreae, M. O., Borrmann, S., and Poschl, U.: Enhanced organic mass fraction and decreased hygroscopicity of cloud condensation nuclei (CCN) during new particle formation events, Geophysical Research Letters, 37, 10.1029/2009gl040930, 2010.

Ehn, M., Thornton, J. A., Kleist, E., Sipila, M., Junninen, H., Pullinen, I., Springer, M., Rubach, F., Tillmann, R., Lee, B., Lopez-Hilfiker, F., Andres, S., Acir, I. H., Rissanen, M., Jokinen, T., Schobesberger, S., Kangasluoma, J., Kontkanen, J., Nieminen, T., Kurten, T., Nielsen, L. B., Jorgensen, S., Kjaergaard, H. G., Canagaratna, M., Dal Maso, M., Berndt, T., Petaja, T., Wahner, A., Kerminen, V. M., Kulmala, M., Worsnop, D. R., Wildt, J., and Mentel, T. F.: A large source of low-volatility secondary organic aerosol, Nature, 506, 476-+, 10.1038/nature13032, 2014.

Frege, C., Bianchi, F., Molteni, U., Trostl, J., Junninen, H., Henne, S., Sipila, M., Herrmann, E., Rossi, M. J., Kulmala, M., Hoyle, C. R., Baltensperger, U., and Dommen, J.: Chemical characterization of atmospheric ions at the high altitude research station Jungfraujoch (Switzerland), Atmos. Chem. Phys., 17, 2613-2629, 10.5194/acp-17-2613-2017, 2017.

Gao, Y., and Anderson, J. R.: Characteristics of Chinese aerosols determined by individual-particle analysis, J. Geophys. Res.-Atmos., 106, 18037-18045, 10.1029/2000jd900725, 2001.

Gong, Z. H., Lan, Z. J., Xue, L., Zeng, L. W., He, L. Y., and Huang, X. F.: Characterization of submicron aerosols in the urban outflow of the central Pearl River Delta region of China, Frontiers of Environmental Science & Engineering, 6, 725-733, 10.1007/s11783-012-0441-8, 2012.

He, L. Y., Huang, X. F., Xue, L., Hu, M., Lin, Y., Zheng, J., Zhang, R. Y., and Zhang, Y. H.: Submicron aerosol analysis and organic source apportionment in an urban atmosphere in Pearl River Delta of China using high-resolution aerosol mass spectrometry, J. Geophys. Res.-Atmos., 116, 10.1029/2010jd014566, 2011.

Hopke, P. K.: Discussion of "Sensitivity of a molecular marker based positive matrix factorization model to the number of receptor observations" by YuanXun Zhang, Rebecca J. Sheesley, Min-Suk Bae and James J. Schauer, Atmos. Environ., 44, 1138-1138, 10.1016/j.atmosenv.2009.12.002, 2010.

Jiang, Q., Sun, Y. L., Wang, Z., and Yin, Y.: Aerosol composition and sources during the Chinese Spring Festival: fireworks, secondary aerosol, and holiday effects,

579 Atmos. Chem. Phys., 15, 6023-6034, 10.5194/acp-15-6023-2015, 2015.
580 Jin, L. Y., Ganopolski, A., Chen, F. H., Claussen, M., and Wang, H. J.: Impacts of
581 snow and glaciers over Tibetan Plateau on Holocene climate change: Sensitivity
582 experiments with a coupled model of intermediate complexity, Geophysical Research
583 Letters, 32, 10.1029/2005gl023202, 2005.
584 Kopacz, M., Mauzerall, D. L., Wang, J., Leibensperger, E. M., Henze, D. K., and
585 Singh, K.: Origin and radiative forcing of black carbon transported to the Himalayas
586 and Tibetan Plateau, Atmos. Chem. Phys., 11, 2837-2852, 10.5194/acp-11-2837-2011,
587 2011.
588 Kumar, A., and Sarin, M. M.: Atmospheric water-soluble constituents in fine and
589 coarse mode aerosols from high-altitude site in western India: Long-range transport
590 and seasonal variability, Atmos. Environ., 44, 1245-1254,
591 10.1016/j.atmosenv.2009.12.035, 2010.
592 Li, C. L., Kang, S. C., Chen, P. F., Zhang, Q. G., Guo, J. M., Mi, J., Basang, P. C.,
593 Luosang, Q. Z., and Smith, K. R.: Personal PM2.5 and indoor CO in nomadic tents
594 using open and chimney biomass stoves on the Tibetan Plateau, Atmos. Environ., 59,
595 207-213, 10.1016/j.atmosenv.2012.05.033, 2012.
596 Li, J. J., Wang, G. H., Wang, X. M., Cao, J. J., Sun, T., Cheng, C. L., Meng, J. J.,
597 Hu, T. F., and Liu, S. X.: Abundance, composition and source of atmospheric PM2.5
598 at a remote site in the Tibetan Plateau, China, Tellus Series B-Chemical and Physical
599 Meteorology, 65, 10.3402/tellusb.v65i0.20281, 2013.
600 Li, W. J., Chen, S. R., Xu, Y. S., Guo, X. C., Sun, Y. L., Yang, X. Y., Wang, Z. F.,
601 Zhao, X. D., Chen, J. M., and Wang, W. X.: Mixing state and sources of submicron
602 regional background aerosols in the northern Qinghai–Tibet Plateau and the influence
603 of biomass burning, Atmos. Chem. Phys., 15, 13365-13376,
604 10.5194/acp-15-13365-2015, 2015.
605 Ma, J. Z., Tang, J., Li, S. M., and Jacobson, M. Z.: Size distributions of ionic
606 aerosols measured at Waliguan Observatory: Implication for nitrate gas-to-particle
607 transfer processes in the free troposphere, J. Geophys. Res.-Atmos., 108,
608 10.1029/2002jd003356, 2003.
609 Masiol, M., Hopke, P. K., Felton, H. D., Frank, B. P., Rattigan, O. V., Wurth, M. J.,
610 and LaDuke, G. H.: Source apportionment of PM2.5 chemically speciated mass and
611 particle number concentrations in New York City, Atmos. Environ., 148, 215-229,
612 https://doi.org/10.1016/j.atmosenv.2016.10.044, 2017.
613 McGregor, G. R.: Climate variability and change in the Sanjiangyuan region, in:
614 Landscape and ecosystem diversity, dynamics and management in the Yellow River
615 Source Zone, Springer, 35-57, 2016.
616 Ming, L., Jin, L., Li, J., Fu, P., Yang, W., Liu, D., Zhang, G., Wang, Z., and Li, X.:
617 PM2.5 in the Yangtze River Delta, China: Chemical compositions, seasonal variations,
618 and regional pollution events, Environ. Pollut., 223, 200-212,
619 https://doi.org/10.1016/j.envpol.2017.01.013, 2017.
620 Mo, Z., Shao, M., Lu, S., Niu, H., Zhou, M., and Sun, J.: Characterization of
621 non-methane hydrocarbons and their sources in an industrialized coastal city, Yangtze
622 River Delta, China, Science of The Total Environment, 593-594, 641-653,

https://doi.org/10.1016/j.scitotenv.2017.03.123, 2017.

Moroni, B., Castellini, S., Crocchianti, S., Piazzalunga, A., Fermo, P., Scardazza, F., and Cappelletti, D.: Ground-based measurements of long-range transported aerosol at the rural regional background site of Monte Martano (Central Italy), Atmospheric Research, 155, 26-36, 10.1016/j.atmosres.2014.11.021, 2015.

Naeher, L. P., Smith, K. R., Leaderer, B. P., Mage, D., and Grajeda, R.: Indoor and outdoor PM2.5 and CO in high- and low-density Guatemalan villages, Journal of Exposure Analysis and Environmental Epidemiology, 10, 544-551, 10.1038/sj.jea.7500113, 2000.

Paatero, P., and Tapper, U.: Positive matrix factorization: A non-negative factor model with optimal utilization of error estimates of data values, Environmetrics, 5, 111-126, 10.1002/env.3170050203, 1994.

Paatero, P.: Least squares formulation of robust non-negative factor analysis, Chemometrics and Intelligent Laboratory Systems, 37, 23-35, http://dx.doi.org/10.1016/S0169-7439(96)00044-5, 1997.

Paatero, P., Hopke, P. K., Song, X.-H., and Ramadan, Z.: Understanding and controlling rotations in factor analytic models, Chemometrics and Intelligent Laboratory Systems, 60, 253-264, http://dx.doi.org/10.1016/S0169-7439(01)00200-3, 2002.

Park, R. J., Jacob, D. J., Field, B. D., Yantosca, R. M., and Chin, M.: Natural and transboundary pollution influences on sulfate-nitrate-ammonium aerosols in the United States: Implications for policy, J. Geophys. Res.-Atmos., 109, 10.1029/2003jd004473, 2004.

Rizzo, M. J., and Scheff, P. A.: Fine particulate source apportionment using data from the USEPA speciation trends network in Chicago, Illinois: Comparison of two source apportionment models, Atmos. Environ., 41, 6276-6288, 10.1016/j.atmosenv.2007.03.055, 2007.

Schulte, P., and Arnold, F.: PYRIDINIUM IONS AND PYRIDINE IN THE FREE TROPOSPHERE, Geophysical Research Letters, 17, 1077-1080, 10.1029/GL017i008p01077, 1990.

Seinfeld, J. H., and Pandis, S. N.: Atmospheric chemistry and physics: from air pollution to climate change, John Wiley & Sons, 2016.

Setyan, A., Song, C., Merkel, M., Knighton, W. B., Onasch, T. B., Canagaratna, M. R., Worsnop, D. R., Wiedensohler, A., Shilling, J. E., and Zhang, Q.: Chemistry of new particle growth in mixed urban and biogenic emissions - insights from CARES, Atmos. Chem. Phys., 14, 6477-6494, 10.5194/acp-14-6477-2014, 2014.

Shen, R. Q., Ding, X., He, Q. F., Cong, Z. Y., Yu, Q. Q., and Wang, X. M.: Seasonal variation of secondary organic aerosol tracers in Central Tibetan Plateau, Atmos. Chem. Phys., 15, 8781-8793, 10.5194/acp-15-8781-2015, 2015.

Su, F. G., Duan, X. L., Chen, D. L., Hao, Z. C., and Cuo, L.: Evaluation of the Global Climate Models in the CMIP5 over the Tibetan Plateau, Journal of Climate, 26, 3187-3208, 10.1175/jcli-d-12-00321.1, 2013.

Sun, Y. L., Wang, Z. F., Fu, P. Q., Yang, T., Jiang, Q., Dong, H. B., Li, J., and Jia, J. J.: Aerosol composition, sources and processes during wintertime in Beijing, China,

667 Atmos. Chem. Phys., 13, 4577-4592, 10.5194/acp-13-4577-2013, 2013.
668 Sun, Y. L., Wang, Z. F., Du, W., Zhang, Q., Wang, Q. Q., Fu, P. Q., Pan, X. L., Li,
669 J., Jayne, J., and Worsnop, D. R.: Long-term real-time measurements of aerosol
670 particle composition in Beijing, China: seasonal variations, meteorological effects,
671 and source analysis, Atmos. Chem. Phys., 15, 10149-10165,
672 10.5194/acp-15-10149-2015, 2015.
673 Tang, J., Wen, Y., Zhou, L., Qi, D., Zheng, M., Trivett, N., and Erika, W.:
674 Observational study of black carbon in clean air area of western China (in Chinese), Q.
675 J. Appl. Meteorol., 10, 160-170, 1999.
676 Tripathee, L., Kang, S. C., Rupakheti, D., Zhang, Q. G., Huang, J., and Sillanpaa,
677 M.: Water-Soluble Ionic Composition of Aerosols at Urban Location in the Foothills
678 of Himalaya, Pokhara Valley, Nepal, Atmosphere, 7, 10.3390/atmos7080102, 2016.
679 Tripathee, L., Kang, S. C., Rupakheti, D., Cong, Z. Y., Zhang, Q. G., and Huang, J.:
680 Chemical characteristics of soluble aerosols over the central Himalayas: insights into
681 spatiotemporal variations and sources, Environ. Sci. Pollut. Res., 24, 24454-24472,
682 10.1007/s11356-017-0077-0, 2017.
683 Valerino, M. J., Johnson, J. J., Izumi, J., Orozco, D., Hoff, R. M., Delgado, R., and
684 Hennigan, C. J.: Sources and composition of PM2.5 in the Colorado Front Range
685 during the DISCOVER-AQ study, J. Geophys. Res.-Atmos., 122, 566-582,
686 10.1002/2016jd025830, 2017.
687 VanCuren, R., and Gustin, M. S.: Identification of sources contributing to PM2.5
688 and ozone at elevated sites in the western US by receptor analysis: Lassen Volcanic
689 National Park, California, and Great Basin National Park, Nevada, Science of the
690 Total Environment, 530, 505-518, 10.1016/j.scitotenv.2015.03.091, 2015.
691 Verma, S. K., Deb, M. K., Suzuki, Y., and Tsai, Y. I.: Ion chemistry and source
692 identification of coarse and fine aerosols in an urban area of eastern central India,
693 Atmospheric Research, 95, 65-76, 10.1016/j.atmosres.2009.08.008, 2010.
694 Wan, X., Kang, S., Wang, Y., Xin, J., Liu, B., Guo, Y., Wen, T., Zhang, G., and
695 Cong, Z.: Size distribution of carbonaceous aerosols at a high-altitude site on the
696 central Tibetan Plateau (Nam Co Station, 4730ma.s.l.), Atmospheric Research, 153,
697 155-164, http://dx.doi.org/10.1016/j.atmosres.2014.08.008, 2015.
698 Wang, G. H., Zhang, R. Y., Gomez, M. E., Yang, L. X., Zamora, M. L., Hu, M.,
699 Lin, Y., Peng, J. F., Guo, S., Meng, J. J., Li, J. J., Cheng, C. L., Hu, T. F., Ren, Y. Q.,
700 Wang, Y. S., Gao, J., Cao, J. J., An, Z. S., Zhou, W. J., Li, G. H., Wang, J. Y., Tian, P.
701 F., Marrero-Ortiz, W., Secrest, J., Du, Z. F., Zheng, J., Shang, D. J., Zeng, L. M.,
702 Shao, M., Wang, W. G., Huang, Y., Wang, Y., Zhu, Y. J., Li, Y. X., Hu, J. X., Pan, B.,
703 Cai, L., Cheng, Y. T., Ji, Y. M., Zhang, F., Rosenfeld, D., Liss, P. S., Duce, R. A.,
704 Kolb, C. E., and Molina, M. J.: Persistent sulfate formation from London Fog to
705 Chinese haze, Proceedings of the National Academy of Sciences of the United States
706 of America, 113, 13630-13635, 10.1073/pnas.1616540113, 2016.
707 Wang, Y., Zhuang, G. S., Tang, A. H., Yuan, H., Sun, Y. L., Chen, S. A., and
708 Zheng, A. H.: The ion chemistry and the source of PM2.5 aerosol in Beijing, Atmos.
709 Environ., 39, 3771-3784, 10.1016/j.atmosenv.2005.03.013, 2005.
710 Wen, Y., Xu, X., Tang, J., Zhang, X., and Zhao, Y.: Enrichment Characteristics

and Origin of Atmospheric Aerosol Elements at Mt Waliguan (in Chinese), Q. J. Appl. Meteorol., 12, 400-408, 2001.

Wu, C. F., Larson, T. V., Wu, S. Y., Williamson, J., Westberg, H. H., and Liu, L. J. S.: Source apportionment of PM2.5 and selected hazardous air pollutants in Seattle, Science of the Total Environment, 386, 42-52, 10.1016/j.scitotenv.2007.07.042, 2007a.

Wu, Z. J., Hu, M., Liu, S., Wehner, B., Bauer, S., Ssling, A. M., Wiedensohler, A., Petaja, T., Dal Maso, M., and Kulmala, M.: New particle formation in Beijing, China: Statistical analysis of a 1-year data set, J. Geophys. Res.-Atmos., 112, 10.1029/2006jd007406, 2007b.

Xu, J., Wang, Z., Yu, G., Qin, X., Ren, J., and Qin, D.: Characteristics of water soluble ionic species in fine particles from a high altitude site on the northern boundary of Tibetan Plateau: Mixture of mineral dust and anthropogenic aerosol, Atmospheric Research, 143, 43-56, http://dx.doi.org/10.1016/j.atmosres.2014.01.018, 2014.

Xu, J. Z., Zhang, Q., Wang, Z. B., Yu, G. M., Ge, X. L., and Qin, X.: Chemical composition and size distribution of summertime PM_{2.5} at a high altitude remote location in the northeast of the Qinghai–Xizang (Tibet) Plateau: insights into aerosol sources and processing in free troposphere, Atmos. Chem. Phys., 15, 5069-5081, 10.5194/acp-15-5069-2015, 2015.

Xu, L., Duan, F., He, K., Ma, Y., Zhu, L., Zheng, Y., Huang, T., Kimoto, T., Ma, T., Li, H., Ye, S., Yang, S., Sun, Z., and Xu, B.: Characteristics of the secondary water-soluble ions in a typical autumn haze in Beijing, Environ. Pollut., 227, 296-305, 10.1016/j.envpol.2017.04.076, 2017.

Yang, K., Wu, H., Qin, J., Lin, C. G., Tang, W. J., and Chen, Y. Y.: Recent climate changes over the Tibetan Plateau and their impacts on energy and water cycle: A review, Global and Planetary Change, 112, 79-91, 10.1016/j.gloplacha.2013.12.001, 2014.

Yao, T., Thompson, L. G., Mosbrugger, V., Zhang, F., Ma, Y., Luo, T., Xu, B., Yang, X., Joswiak, D. R., Wang, W., Joswiak, M. E., Devkota, L. P., Tayal, S., Jilani, R., and Fayziev, R.: Third Pole Environment (TPE), Environmental Development, 3, 52-64, http://dx.doi.org/10.1016/j.envdev.2012.04.002, 2012.

Yao, X. H., Chan, C. K., Fang, M., Cadle, S., Chan, T., Mulawa, P., He, K. B., and Ye, B. M.: The water-soluble ionic composition of PM2.5 in Shanghai and Beijing, China, Atmos. Environ., 36, 4223-4234, 10.1016/s1352-2310(02)00342-4, 2002.

Zhang, N., Cao, J., Liu, S., Zhao, Z., Xu, H., and Xiao, S.: Chemical composition and sources of PM2.5 and TSP collected at Qinghai Lake during summertime, Atmospheric Research, 138, 213-222, 10.1016/j.atmosres.2013.11.016, 2014.

Zhang, N. N., Cao, J. J., Ho, K. F., and He, Y. Q.: Chemical characterization of aerosol collected at Mt. Yulong in wintertime on the southeastern Tibetan Plateau, Atmospheric Research, 107, 76-85, 10.1016/j.atmosres.2011.12.012, 2012.

Zhang, T., Cao, J. J., Tie, X. X., Shen, Z. X., Liu, S. X., Ding, H., Han, Y. M., Wang, G. H., Ho, K. F., Qiang, J., and Li, W. T.: Water-soluble ions in atmospheric aerosols measured in Xi'an, China: Seasonal variations and sources, Atmospheric

Research, 102, 110-119, https://doi.org/10.1016/j.atmosres.2011.06.014, 2011.

Zhang, Y., Zhang, H., Deng, J., Du, W., Hong, Y., Xu, L., Qiu, Y., Hong, Z., Wu, X., Ma, Q., Yao, J., and Chen, J.: Source regions and transport pathways of PM2.5 at a regional background site in East China, Atmos. Environ., 167, 202-211, https://doi.org/10.1016/j.atmosenv.2017.08.031, 2017.

Zhao, P. S., Dong, F., He, D., Zhao, X. J., Zhang, X. L., Zhang, W. Z., Yao, Q., and Liu, H. Y.: Characteristics of concentrations and chemical compositions for PM2.5 in the region of Beijing, Tianjin, and Hebei, China, Atmos. Chem. Phys., 13, 4631-4644, 10.5194/acp-13-4631-2013, 2013a.

Zhao, Z. Z., Cao, J. J., Shen, Z. X., Xu, B. Q., Zhu, C. S., Chen, L. W. A., Su, X. L., Liu, S. X., Han, Y. M., Wang, G. H., and Ho, K. F.: Aerosol particles at a high-altitude site on the Southeast Tibetan Plateau, China: Implications for pollution transport from South Asia, J. Geophys. Res.-Atmos., 118, 11360-11375, 10.1002/jgrd.50599, 2013b.

Zhao, Z. Z., Cao, J. J., Shen, Z. X., Huang, R. J., Hu, T. F., Wang, P., Zhang, T., and Liu, S. X.: Chemical composition of PM2.5 at a high-altitude regional background site over Northeast of Tibet Plateau, Atmos. Pollut. Res., 6, 815-823, 10.5094/apr.2015.090, 2015.

Zhou, L. M., Hopke, P. K., Stanier, C. O., Pandis, S. N., Ondov, J. M., and Pancras, J. P.: Investigation of the relationship between chemical composition and size distribution of airborne particles by partial least squares and positive matrix factorization, J. Geophys. Res.-Atmos., 110, 10.1029/2004jd005050, 2005.

Zhou, Y., Wang, T., Gao, X. M., Xue, L. K., Wang, X. F., Wang, Z., Gao, J. A., Zhang, Q. Z., and Wang, W. X.: Continuous observations of water-soluble ions in PM2.5 at Mount Tai (1534 ma.s.l.) in central-eastern China, Journal of Atmospheric Chemistry, 64, 107-127, 10.1007/s10874-010-9172-z, 2009.